ARTICLE

Carbon Nanotube Photo- and Electroluminescence in Longitudinal Electric Fields

Marcus Freitag,* Mathias Steiner, Anton Naumov,† Joshua P. Small, Ageeth A. Bol, Vasili Perebeinos, and Phaedon Avouris

IBM Thomas J. Watson Research Center, Yorktown Heights, New York 10598. †Permanent address: Applied Physics Program, Rice University, Houston, Texas 77005.

ABSTRACT The photoluminescence of a partially suspended, semiconducting carbon nanotube that forms the active channel of a field-effect transistor is quenched and red-shifted upon application of a longitudinal electrical (source−drain) field. The quenching can be explained by a loss of oscillator strength and an increased Auger-like nonradiative decay of the E_{11} exciton. The spectral shifts are due to drain-field-induced doping that leads to enhanced dielectric screening. Electroluminescence due to electron impact excitation of E_{11} excitons is red-shifted and broadened with respect to the zero-field photoluminescence. A combination of screening and heating of the carbon nanotube can explain both spectral shift and broadening of the electrically induced light emission.

KEYWORDS: carbon nanotube · field-effect transistor · excitons · doping · screening · photoluminescence · electroluminescence · optoelectronics · nanophotonics

*Address correspondence to mfreitag@us.ibm.com.

Received for review August 7, 2009 and accepted October 18, 2009.

Published online October 29, 2009. 10.1021/nn900962f CCC: $40.75

Light emission in semiconducting single-wall carbon nanotubes (CNTs) results from the radiative decay of E_{11} excitons[1−3] and depends strongly on the CNT diameter[4] and dielectric environment.[5−8] Theoretical work suggests field ionization and Stark shifts of excitons in CNTs in longitudinal electric fields.[9] In previous studies, the photoluminescence (PL) intensity was shown to drop in longitudinal electric fields.[10,11] Spectral shifts of up to 4 meV were observed for some CNTs.[11] Light emission in CNTs can also be induced by an electrical current.[12] In suspended CNTs, this electroluminescence (EL) is due to a unipolar transport current that produces excitons *via* impact excitation.[13,14] The dependence of the EL intensity on the source−drain field is threshold-like.[13] While room-temperature PL from CNTs has spectral widths of ∼20 meV (fwhm),[15] EL under high-field conditions is much broader (100−300 meV).[16,17] Up to now, there has been no direct comparison of PL and EL spectra from the same CNT, and it is unclear whether the EL is energetically up- or down-shifted with respect to the PL. Hot carrier luminescence would suggest a blue shift,[16] while heating effects,[15] a DC Stark effect,[9] or electrostatic field doping[18] would suggest red shifts. Here we show that EL is red-shifted by several tens of millielectronvolts with respect to the zero-field PL, and self-heating of the CNT is responsible for the broadening of the EL spectrum. The drain voltage induces strong quenching and spectral red shifts in the PL spectra of suspended CNTs. The PL results are explained in the context of drain-induced doping of the CNT that leads to a loss of oscillator strength due to band-filling and screening as well as an increase in Auger-type nonradiative decay of the excitons. Spectral shifts due to the polarization of the excitons (dc Stark effect) and quenching due to exciton ionization are negligible compared to doping-related effects.

RESULTS AND DISCUSSION

The inset of Figure 1a shows a scanning electron microscope image of the suspended CNT field-effect transistor (FET). Details regarding device fabrication and measurements can be found in the Methods section. Longitudinal electric fields are generated by applying a voltage V_{DS} between source and drain electrodes. The electrical transport (I_{DS},V_{DS}) characteristics of the CNT transistor are shown in Figure 1a for several values of the gate voltage V_G. The device shows unipolar (hole) transport, and the ratio between the drain−source currents I_{DS} in on- and off-states spans 4 orders of magnitude.

Resonance-Raman scattering intensities of CNTs[19,20] depend on the charge carrier density (or doping level) ρ of the CNT.[18,21−24] In order to probe changes of ρ as a function of V_G and V_{DS}, we record the intensity of the Raman G-band, and the results are shown in the inset of Figure 1b. We find that both positive and negative gate

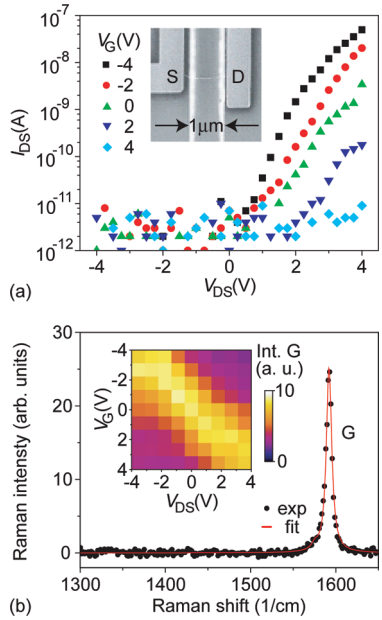

Figure 1. (a) Electrical transport (I_{DS}) characteristics of the partially suspended carbon nanotube field-effect transistor (CNT-FET). The transport current is p-type because of doping by the substrate in the supported CNT segments. (Inset) SEM image of the CNT partially suspended between the metallic source (S) and drain (D) electrodes and partially supported by the SiO_2 substrate. The back gate (G) is formed by a Si layer beneath. (b) G-band Raman spectrum of the CNT excited at λ_{laser} = 566.7 nm. (Inset) G-band intensity as functions of drain−source voltage V_{DS} and gate voltage V_G. The laser wavelength is λ_{laser} = 582.25 nm, which is close to the E_{33} resonance of the CNT. The suspended part of the CNT is intrinsic at $V_G = V_{DS} = 0$ V and can be doped n- or p-type by either V_G or V_{DS}.

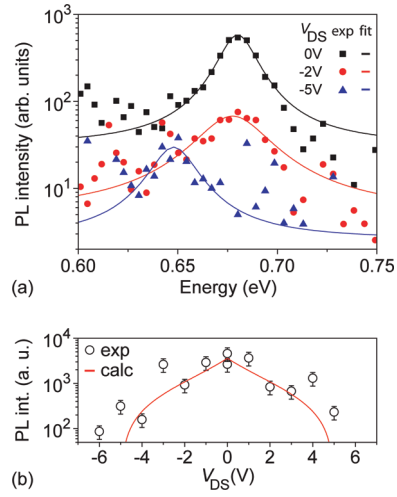

Figure 2. (a) Three representative photoluminescence (PL) spectra of the CNT for different drain−source voltages V_{DS}, all excited at λ_{laser} = 514.5 nm. (b) Integrated PL intensity plotted as a function of the drain−source voltage V_{DS}. The red solid curve is a model calculation based on eq 3.

voltages strongly reduce the measured Raman intensities for laser excitation energies close to the E_{33} resonance of the CNT near 2.2 eV.[18] This indicates that the suspended part of the CNT is intrinsic at $V_G = 0$ V. Importantly, changes in drain voltage also affect the doping level of the CNT. As can be seen in the inset of Figure 1b, the effect of a positive (negative) gate voltage can be reversed by applying a positive (negative) drain voltage.

In a simple picture, we would expect that the drain-induced doping of the suspended CNT segment is only half as efficient as the doping induced by the gate, that is, $\rho(V_{DS}) \approx \rho(V_G/2)$, because the source contact stays at 0 V throughout the measurements. However, when the contact resistances of source and drain are different, the efficiency ratio can vary anywhere between 0 and 1. In the present case, we find that doping induced by the drain is nearly as efficient as doping by the gate, that is, $\rho(V_{DS}) \approx \rho(V_G)$, as is evident from the symmetric, diagonal Raman intensity pattern (see inset in Figure 1b). The fact that the electrical transport characteristic is p-type, even though the suspended part of the CNT is ambipolar, can be understood in a simple series model, where the supported CNT segments limit the transport current for positive gate voltages. For negative gate voltages, both supported and suspended CNT segments are in the on-state and we observe (hole) currents of up to several hundred nanoamperes.

In the following, we investigate the drain voltage dependence of the PL spectrum (Figure 2). For increasing $|V_{DS}|$, we observe a substantial drop of PL intensity and a noticeable red shift of the E_{11} peak energy. A quenching mechanism that can cause the drop of PL intensity could be field-induced ionization of E_{11} excitons into a continuum of single-particle states. The ionization rate Γ scales exponentially with the longitudinal electric field F_{DS}:

$$\Gamma = 4.1E_b\frac{F_0}{F_{DS}}\exp\left(-\frac{F_0}{F_{DS}}\right) \quad (1)$$

where E_b is the exciton binding energy, $F_0 \approx 1.74E_b^{3/2}m_{exc}^{1/2}/e\hbar$, and m_{exc} is the reduced exciton mass.[9] In the present case, $m_{exc} = \Delta/2v_F^2 \approx 0.026m_e$, where m_e is the electron mass, $v_F = 10^6$ m/s is the Fermi velocity, $\Delta(\approx 0.42\ \text{eV}/d_t)$ is half of the single particle band gap energy and d_t = 1.4 nm. We estimate E_b in the freely suspended CNT with d_t = 1.4 nm to be around 0.45 eV by referring to results from *ab initio* calculations for an (8,0) CNT with E_b = 1 eV[25] and by accounting for the $1/d$ scaling of E_b.[5,26] This estimate delivers F_0 = 307 V/μm. As a result, even for the highest source−drain fields of $|F_{DS}| \approx$ 6 V/μm, we find that $\Gamma = 10^{-20}$ eV is extremely small and cannot be responsible for the measured PL intensity drop.

Alternatively, the drop of the integrated PL intensity could be associated with changes in the dielectric screening due to drain-induced doping of the CNT. In order to quantify the PL intensity changes, we have to consider changes in the PL quantum yield

$$Q = k_r/(k_r + k_{nr}) \quad (2)$$

where k_r and k_{nr} are the radiative and nonradiative exciton recombination rates, respectively. The effects can be summarized as follows: (I) Filling of a free-carrier band, which reduces the free-carrier oscillator strength f_{free} and, hence, the E_{11} exciton oscillator strength $f_{exciton} = \eta \times f_{free}(\rho)$. Here, η describes the transfer of oscillator strength from free carriers to the bound exciton state. (II) Enhanced exciton screening,[5] which leads to a loss of E_{11} oscillator strength because $\eta(\varepsilon,\rho)$ decreases with increasing $|\rho|$. (III) Auger-like nonradiative decay[27] involving an exciton, a free carrier (hole), and emission of an optical phonon.[28] While (I) and (II) decrease k_r, (III) increases k_{nr}. For small field-induced perturbations, all of these changes are expected to be linear in the charge carrier density ρ.

The gate dependence of the photoluminescence intensity of the same CNT-FET has been discussed already in detail in ref 18, and we estimated there that the change of the CNT absorption strength at $E_{laser} = 2.4$ eV does not exceed a factor of 2 and, hence, has only a minor influence on the observed PL intensity dependence. On the basis of our previous findings and the results shown in Figure 1b, we use an effective gate voltage $V_{G,eff} = V_{DS}$ in order to model the data in Figure 2b according to

$$I_{PL} = I_{PL,0V}\frac{1 - aV_{G,eff}}{1 + bV_{G,eff}} \quad (3)$$

Here, changes in the radiative decay rate from the zero-field value k_r^0 are captured in the coefficient a, while changes in the nonradiative rate k_{nr}^0 are captured in b. The coefficients $a = 0.2\ V^{-1}$ and $b = 0.5\ V^{-1}$ are taken from the best fit of the gate voltage dependence of the integrated PL intensity of the same CNT-FET,[18] and their sum represents the overall drop of the measured zero-field PL intensity $I_{PL,0V}$. Note that there are no adjustable parameters in the modeled curve shown in Figure 2b. From the good agreement of the experimental data with the predictions of this simple model, we conclude that drain-induced doping is the major mechanism responsible for the measured PL intensity drop.

The spectral peak positions of the E_{11} photoluminescence band of the CNT as a function of V_{DS} are shown in Figure 3. We obtain red shifts of up to 30 meV at $|V_{DS}| = 6$ V. A dc Stark effect induced by the longitudinal field could, in principle, be responsible for the observed red shift. On the basis of the relation $\kappa_{dc} = -3.4e^2d^2/E_b$[28] and assuming an exciton binding energy $E_b = 0.45$ eV, we estimate $\kappa_{dc} = -1.48 \times 10^{-17}\ m^2\ eV^{-1}$, which translates into a dc Stark shift of about $\Delta E_{11} = 0.5$ meV at $|V_{DS}| = 6$ V. This is 2 orders of magnitude smaller than the experimental shifts shown in Figure 3 and therefore cannot explain our observations.

Another possibility is that the E_{11} energy shifts are due to drain-induced doping, in analogy to the E_{33} exciton red shifts observed upon field-doping induced by the gate field.[18] In this scenario, the screening of the Coulomb interaction in the CNT increases with the doping level and would be responsible for both a renormalization of the band gap and a reduction of the exciton binding energy.[8] Following the procedure in ref 18 and using $V_{G,eff} = V_{DS}$, we estimate the doping level ρ in the CNT following[29] by using

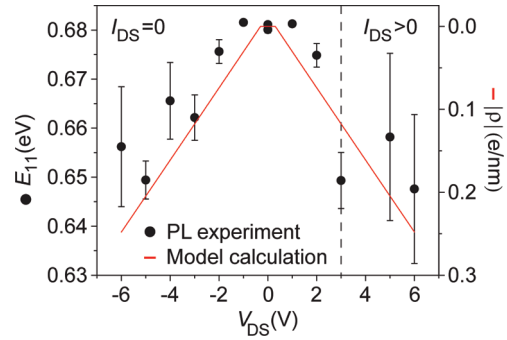

Figure 3. E_{11} peak energy obtained from the measured PL band as a function of the drain−source voltage V_{DS}. Electrical transport I_{DS} turns on around $V_{DS} = 3$ V (dashed line) and deteriorates the signal-to-noise ratio of the PL measurement. The graph is overlaid with a plot of the charge carrier density ρ in the CNT as a function of V_{DS} that has been modeled based on eq 4.

$$V_{G,eff} = E_F/e + \rho/C_{G,eff},\quad C_G = 2\pi\varepsilon_0\varepsilon/\ln(4t/d_t) \quad (4)$$

Here, $C_G = 0.07$ pF/cm is the electrostatic gate capacitance that was estimated based on the vacuum dielectric constant ε_0, the dielectric constant of air $\varepsilon = 1$, the thickness of the gate dielectric $t = 1000$ nm, and $d_t = 1.4$ nm. Furthermore, $E_F = \Delta + \hbar^2 v_F^2 k_F^2/2\Delta$ is the Fermi energy and $k_F = \pi\rho/4$ is the Fermi wave vector. On the basis of this approach, we obtain a maximum charge carrier density of $|\rho| = 0.25$ e/nm at $|V_{DS}| = 6$ V.

In Figure 3, we overlay the plot of the experimental E_{11} peak energies with a curve of the charge carrier density ρ as a function of V_{DS} that has been modeled based on eq 4. By comparing the two curves, we obtain the scaling relation $\Delta E_{11}/\Delta|\rho| = -0.12$ eV/(e/nm). The measured shifts of the E_{11} transition energy are of the same order of magnitude as the E_{33} red shifts that we observed for the same CNT upon electrostatic doping induced by the gate field.[18] Comparable E_{ii} shifts have also been obtained through changes in the dielectric screening in CNTs induced by interface modifications.[30,31]

Under high-field conditions ($V_{DS} = 7$ V, $V_G = -6$ V, $I_{DS} = 350$ nA), we are able to measure the EL spectrum of the CNT and compare it to the zero-field PL spectrum in Figure 4. Unlike the PL signal that drops dramatically if external electric fields are applied (see Figure 2), the unipolar EL emission relies on high external fields in the first place and exhibits threshold-like electrical power dependence.[13] As compared to the zero-field PL, we observe a red shift of 40 meV and a 5-fold broadening of the E_{11} peak. The shift is of the same order of

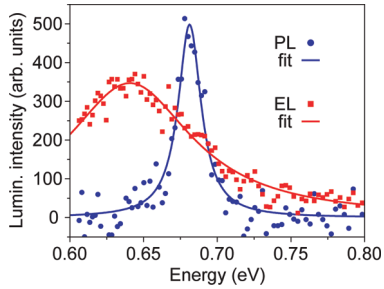

Figure 4. Photoluminescence (PL; peak energy = 0.68 eV, width = 20 meV) and electroluminescence (EL; peak energy = 0.64 eV, width = 100 meV) spectrum of the same CNT. The PL is excited at 2.41 eV, just above the E_{33} resonance (2.2 eV), with a laser power density of 30kW/cm^2. The EL is driven at V_{DS} = 7 V, V_G = −6 V, and I_{DS} = 350 nA, resulting in an electrical power of 2.45 μW.

magnitude as the E_{11} peak shift for the highest drain−source voltages $|V_{DS}|$ in our PL experiment (see Figure 3). The red shift of the E_{11} peak in EL can therefore be attributed to the same cause: enhanced screening as a result of drain-induced doping. In addition, the electrical power dissipation heats the CNT to temperatures of ~1000 K at high biases,[32] which is responsible for the 5-fold broadening of the electroluminescence as compared to PL experiments where thermal effects are negligible. In the current saturation regime, where the electron temperature exceeds the phonon temperatures,[33] further broadening of the emission spectrum is expected.

In conclusion, our results show that changes in screening induced by electrostatic fields have to be taken into account in analyzing CNT-based optoelectronic devices. Strong quenching of the PL emission in external electrostatic fields is caused by the filling of the free-particle band that decreases the oscillator strength and increases Auger-type nonradiative decay of the E_{11} exciton. Doping-related screening simultaneously red shifts the E_{11} transition energy by up to 30 meV. In unipolar EL, charge carriers need to be accelerated by external fields to excite electron−hole pairs (excitons). As a result, the EL emission is only observable at high external fields and red-shifted by several tens of millielectronvolts with respect to the zero-field PL of the same CNT. The 5-fold current-induced broadening of the EL spectrum with respect to the zero-field PL is caused by hot electrons and phonons in the CNT.

METHODS

Sample Fabrication. CNTs were grown by CVD across a trench (width = 1 μm, depth = 750 nm) in a SiO_2 layer (thickness = 1 μm) on top of a silicon wafer. Both ends of an individual CNT (diameter d_t = 1.4 nm as determined by Raman spectroscopy)[18] were covered by metal contacts close to the edges of the trench (see inset of Figure 1a). Electron beam lithography was used to define the contacts, and the lift-off was followed by critical-point drying. The suspended part of the nanotube was not exposed to the electron beam during the lithography because we used a positive e-beam resist (PMMA). We did use SEM to locate bridging nanotubes over the trench, but the exposure was kept short and at a low dose (low magnification) to avoid damaging the nanotube or changing its light-emitting properties.

Micro-Raman Spectroscopy. Raman spectra were excited using a tunable dye laser (CR-599 operated with R6G solution, Coherent) operated between 561 and 588 nm. The light was focused with a microscope objective (100×, NA = 0.8, Nikon) onto the suspended part of the CNT-FET (focal spot diameter around 500 nm). Excitation power densities were kept below 100 kW/cm^2 to avoid heating of the tube. The Raman scattered light was collected by the same objective and sent through a Notch filter and into a spectrometer (Triax 322 Horiba Jobin Yvon), equipped with a 1200 mm^{-1} groove density 500 nm blaze grating and a LN_2-cooled CCD. The sample was positioned with a closed-loop piezo-electric scanning stage (P-527.2CL, Physik Instrumente).

Photoluminescence (PL) and Electroluminescence (EL) Spectroscopy. The PL of the CNT was excited at 514.5 nm using an Ar^+ laser (Innova 300, Coherent) with excitation power densities of the order of 30 kW/cm^2. A microscope objective (100×, NA = 0.8, Nikon) was used to focus the incoming and collect the outgoing light. The PL emission was sent through a long-pass filter and a transmission grating (fabricated on top of a prism) and into a LN_2-cooled two-dimensional HgCdTe detector array (IRLabs). The spectroscopic unit was calibrated using suitable band-pass filters. During the PL measurements, longitudinal electric fields were generated by applying a voltage V_{DS} between source and drain electrodes (see inset Figure 1a). Unipolar EL emission of the same CNT was produced by running a hole current of 350 nA (V_{DS} = 7 V, V_G = −6 V) through the CNT and detected with the same spectroscopic setup that was used for the PL spectroscopy.

REFERENCES AND NOTES

1. Ando, T. Excitons in Carbon Nanotubes. *J. Phys. Soc. Jpn.* **1997**, *66*, 1066–1073.
2. Wang, F.; Dukovic, G.; Brus, L. E.; Heinz, T. F. The Optical Resonances in Carbon Nanotubes Arise from Excitons. *Science* **2005**, *308*, 838–841.
3. Maultzsch, J.; Pomraenke, R.; Reich, S.; Chang, E.; Prezzi, D.; Ruini, A.; Molinari, E.; Strano, M. S.; Thomsen, C.; Lienau, C. Exciton Binding Energies in Carbon Nanotubes from Two-Photon Photoluminescence. *Phys. Rev. B* **2005**, *72*, 241402–241404.
4. Bachilo, S. M.; Strano, M. S.; Kittrell, C.; Hauge, R. H.; Smalley, R. E.; Weisman, R. B. Structure-Assigned Optical Spectra of Single-Walled Carbon Nanotubes. *Science* **2002**, *298*, 2361–2366.
5. Perebeinos, V.; Tersoff, J.; Avouris, P. Scaling of Excitons in Carbon Nanotubes. *Phys. Rev. Lett.* **2004**, *92*, 257402.
6. Hertel, T.; Hagen, A.; Talalaev, V.; Arnold, K.; Hennrich, F.; Kappes, M.; Rosenthal, S.; McBride, J.; Ulbricht, H.; Flahaut, E. Spectroscopy of Single- and Double-Wall Carbon Nanotubes in Different Environments. *Nano Lett.* **2005**, *5*, 511–514.
7. Heller, D. A.; Jeng, E. S.; Yeung, T.-K.; Martinez, B. M.; Moll, A. E.; Gastala, J. B.; Strano, M. S. Optical Detection of DNA Conformational Polymorphism on Single-Walled Carbon Nanotubes. *Science* **2006**, *311*, 508–511.
8. Avouris, P.; Freitag, M.; Perebeinos, V. Carbon-Nanotube Photonics and Optoelectronics. *Nat. Photonics* **2008**, *2*, 341–350.
9. Perebeinos, V.; Avouris, P. Exciton Ionization, Franz-Keldysh, and Stark Effects in Carbon Nanotubes. *Nano Lett.* **2007**, *7*, 609–613.
10. Ohno, Y.; Kishimoto, S.; Mizutani, T. Photoluminescence of Single-Walled Carbon Nanotubes in Field-Effect Transistors. *Nanotechnology* **2006**, *17*, 549–555.

11. Naumov, A. V.; Bachilo, S. M.; Tsyboulski, D. A.; Weisman, R. B. Electric Field Quenching of Carbon Nanotube Photoluminescence. *Nano Lett.* **2008**, *8*, 1527–1531.
12. Misewich, J. A.; Martel, R.; Avouris, P.; Tsang, J. C.; Heinze, S.; Tersoff, J. Electrically Induced Optical Emission from a Carbon Nanotube FET. *Science* **2003**, *300*, 783–786.
13. Chen, J.; Perebeinos, V.; Freitag, M.; Tsang, J.; Fu, Q.; Liu, J.; Avouris, P. Bright Infrared Emission from Electrically Induced Excitons in Carbon Nanotubes. *Science* **2005**, *310*, 1171–1174.
14. Freitag, M.; Tsang, J. C.; Kirtley, J.; Carlsen, A.; Chen, J.; Troeman, A.; Hilgenkamp, H.; Avouris, P. Electrically Excited, Localized Infrared Emission from Single Carbon Nanotubes. *Nano Lett.* **2006**, *6*, 1425–1433.
15. Lefebvre, J.; Finnie, P.; Homma, Y. Temperature-Dependent Photoluminescence from Single-Walled Carbon Nanotubes. *Phys. Rev. B* **2004**, *70*, 045419.
16. Freitag, M.; Perebeinos, V.; Chen, J.; Stein, A.; Tsang, J. C.; Misewich, J. A.; Martel, R.; Avouris, P. Hot Carrier Electroluminescence from a Single Carbon Nanotube. *Nano Lett.* **2004**, *4*, 1063–1066.
17. Xia, F.; Steiner, M.; Lin, Y.-m.; Avouris, P. A. Microcavity-Controlled, Current-Driven, On-Chip Nanotube Emitter at Infrared Wavelengths. *Nat. Nano.* **2008**, *3*, 609–613.
18. Steiner, M.; Freitag, M.; Perebeinos, V.; Naumov, A.; Small, J. P.; Bol, A. A.; Avouris, P. Gate-Variable Light Absorption and Emission in a Semiconducting Carbon Nanotube. *Nano Lett.* **2009**, *9*, 3477−3481.
19. Dresselhaus, M. S.; G. Dresselhaus, G.; R. Saito, R.; Jorio, A. Raman Spectroscopy of Carbon Nanotubes. *Phys. Rep.* **2005**, *409*, 47–99.
20. Thomsen, C.; Reich, S. Raman Scattering in Carbon Nanotubes. In *Light Scattering in Solid IX*; Cardona, M., Merlin, R., Eds.; Springer: Berlin/Heidelberg, 2007; Vol. 108, pp 115−234.
21. Cronin, S. B.; Barnett, R.; Tinkham, M.; Chou, S. G.; Rabin, O.; Dresselhaus, M. S.; Swan, A. K.; Unlu, M. S.; Goldberg, B. B. Electrochemical Gating of Individual Single-Wall Carbon Nanotubes Observed by Electron Transport Measurements and Resonant Raman Spectroscopy. *Appl. Phys. Lett.* **2004**, *84*, 2052–2054.
22. Kavan, L.; Rapta, P.; Dunsch, L.; Bronikowski, M. J.; Willis, P.; Smalley, R. E. Electrochemical Tuning of Electronic Structure of Single-Walled Carbon Nanotubes: *In-Situ* Raman and Vis−NIR Study. *J. Phys. Chem. B* **2001**, *105*, 10764–10771.
23. Stoll, M.; Rafailov, P. M.; Frenzel, W.; Thomsen, C. Electrochemical and Raman Measurements on Single-Walled Carbon Nanotubes. *Chem. Phys. Lett.* **2003**, *375*, 625–631.
24. Corio, P.; Jorio, A.; Demir, N.; Dresselhaus, M. S. Spectro-Electrochemical Studies of Single Wall Carbon Nanotubes Films. *Chem. Phys. Lett.* **2004**, *392*, 396–402.
25. Spataru, C. D.; Ismail-Beigi, S.; Benedict, L. X.; Louie, S. G. Excitonic Effects and Optical Spectra of Single-Walled Carbon Nanotubes. *Phys. Rev. Lett.* **2004**, *92*, 077402-4.
26. Dukovic, G.; Wang, F.; Song, D.; Sfeir, M. Y.; Heinz, T. F.; Brus, L. E. Structural Dependence of Excitonic Optical Transitions and Band-Gap Energies in Carbon Nanotubes. *Nano Lett.* **2005**, *5*, 2314–2318.
27. Wang, F.; Dukovic, G.; Knoesel, E.; Brus, L. E.; Heinz, T. F. Observation of Rapid Auger Recombination in Optically Excited Semiconducting Carbon Nanotubes. *Phys. Rev. B* **2004**, *70*, 241403.
28. Perebeinos, V.; Avouris, P. Phonon and Electronic Nonradiative Decay Mechanisms of Excitons in Carbon Nanotubes. *Phys. Rev. Lett.* **2008**, *101*, 057401-4.
29. Datta, S. *Quantum Transport: Atom to Transistor*; Cambridge University Press: Cambridge, 2005.
30. Walsh, A. G.; Vamivakas, A. N.; Yin, Y.; Cronin, S. B.; Unlu, M. S.; Goldberg, B. B.; Swan, A. K. Screening of Excitons in Single, Suspended Carbon Nanotubes. *Nano Lett.* **2007**, *7*, 1485–1488.
31. Steiner, M.; Freitag, M.; Tsang, J.; Perebeinos, V.; Bol, A.; Failla, A.; Avouris, P. How Does the Substrate Affect the Raman and Excited State Spectra of a Carbon Nanotube? *Appl. Phys. A: Mater. Sci. Process.* **2009**, *96*, 271–282.
32. Steiner, M.; Freitag, M.; Perebeinos, V.; Tsang, J. C.; Small, J. P.; Kinoshita, M.; Yuan, D.; Liu, J.; Avouris, P. Phonon Populations and Electrical Power Dissipation in Carbon Nanotube Transistors. *Nat. Nano.* **2009**, *4*, 320–324.
33. Pop, E.; Mann, D.; Cao, J.; Wang, Q.; Goodson, K.; Dai, H. Negative Differential Conductance and Hot Phonons in Suspended Nanotube Molecular Wires. *Phys. Rev. Lett.* **2005**, *95*, 155505.